Neuroscience 319 (2016) 92–106

A RANDOMIZED, PLACEBO-CONTROLLED TRIAL OF THE BENZOQUINONE IDEBENONE IN A MOUSE MODEL OF OPA1-RELATED DOMINANT OPTIC ATROPHY REVEALS A LIMITED THERAPEUTIC EFFECT ON RETINAL GANGLION CELL DENDROPATHY AND VISUAL FUNCTION

T. G. SMITH,[a] S. SETO,[a] P. GANNE[b] AND M. VOTRUBA[a,c]*

[a] *School of Optometry and Vision Sciences, Cardiff University, Maindy Road, Cardiff CF24 4HQ, United Kingdom*

[b] *Ipswich Hospital NHS Trust, Heath Road, Ipswich IP4 5PD, United Kingdom*

[c] *Cardiff Eye Unit, University Hospital Wales, Heath Park, Cardiff CF14 4XN, United Kingdom*

Abstract—Dominant optic atrophy (DOA) arises from mutations in the *OPA1* gene that promotes fusion of the inner mitochondrial membrane and plays a role in maintaining ATP levels. Patients display optic disc pallor, retinal ganglion cell (RGC) loss and bilaterally reduced vision. We report a randomized, placebo-controlled trial of idebenone at 2000 mg/kg/day in 56 *Opa1* mutant mice (B6;C3-*Opa1*^{Q285STOP}), with RGC dendropathy and visual loss, and 63 wildtype mice. We assessed cellular responses in the retina, brain and liver and RGC morphology, by diolistic labeling, Sholl analysis and quantification of dendritic morphometric features. Vision was assessed by optokinetic responses. ATP levels were raised by 0.57 nmol/mg (97.73%, $p = 0.035$) in brain from idebenone-treated *Opa1* mutant mice, but in the liver there was an 80.35% ($p = 0.011$) increase in oxidative damage. NQO1 expression in *Opa1* mutant mice was reduced in the brain (to 30.5%, $p = 0.002$) but not in retina, and neither expression level was induced by idebenone. ON-center RGCs failed to show major recovery, other than improvements in secondary dendritic length (by 53.89%, $p = 0.052$) and dendritic territory (by 2.22×10^4 μm^2 or 90.24%, $p = 0.074$). An improvement in optokinetic response was observed (by 12.2 ± 3.2 s, $p = 0.003$), but this effect was not sustained over time. OFF-center RGCs from idebenone-treated wildtype mice showed shrinkage in total dendritic length by 2.40 mm (48.05%, $p = 0.025$) and a 47.37% diminished Sholl profile ($p = 0.029$). Visual function in wildtype idebenone-treated mice was impaired (2.9 fewer head turns than placebo, $p = 0.007$). Idebenone appears largely ineffective in protecting *Opa1* heterozygous RGCs from dendropathy. The detrimental effect of idebenone in wildtype mice has not been previously observed and raises some concerns.

Key words: dominant optic atrophy, idebenone, NQO1, retinal ganglion cell, OPA1, mitochondria.

INTRODUCTION

Dominant optic atrophy is a mitochondrial optic neuropathy that can affect between 1 in 30,000 and 1 in 10,000 people, and manifests as a loss of retinal ganglion cells and reduction in visual acuity leading to blindness (Votruba et al., 1998b; Newman and Biousse, 2004). There is no current treatment, although idebenone has been proposed as a potential therapy (Yu-Wai-Man et al., 2014). Recently idebenone has been given approval by the European Medicines Agency for use in patients with another mitochondrial optic neuropathy, Leber's hereditary optic neuropathy (http://www.ema.europa.eu/ema/), making a trial of idebenone in dominant optic atrophy very logical and topical. Patients with dominant optic atrophy present with reduction in best-corrected visual acuities ranging from light perception to 20/20 (median 20/120) (Votruba et al., 1998a), and a subset of patients may also develop peripheral neuropathies, myopathies and sensorineural hearing loss (Yu-Wai-Man et al., 2010; Chao de la Barca et al., 2015). The majority of cases derive from dominantly inherited somatic mutations in the optic atrophy locus 1 gene (*OPA1*) located on chromosome 3q28 (Eiberg et al., 1994; Alexander et al., 2000; Delettre et al., 2000) although mutations in other genes can cause inherited optic neuropathies resembling dominant optic atrophy (Lenaers et al., 2012). The *OPA1* gene encodes a small GTPase of the dynamin family, and following the proteolytic cleavage of the OPA1 protein it functions as a pro-fusion factor in the inner mitochondrial membrane (Davies and Votruba, 2006; Song et al., 2007; Alavi and Fuhrmann, 2013). Skin fibroblasts and peripheral blood lymphocytes from dominant optic atrophy patients reveal reduced levels of

*Correspondence to: M. Votruba, School of Optometry and Vision Sciences, Cardiff University, Maindy Road, Cardiff CF24 4HQ, United Kingdom.
E-mail address: VotrubaM@cardiff.ac.uk (M. Votruba).

Abbreviations: DiI, 1,1′-dioctadecyl-3,3,3′,3′-tetramethylindocarbocyanine perchlorate; GLC, ganglion cell layer; INL, inner nuclear layer; IS, inner segment of photoreceptive layer; NQO1, NAD(P)H:quinone oxidoreductase-1; ONL, outer nuclear layer; TBARS, thiobarbituric acid reactive species.

http://dx.doi.org/10.1016/j.neuroscience.2016.01.042
0306-4522/

OPA1 protein associated with defective mitochondrial fusion and increased mitochondrial fission (Agier et al., 2012), with increased susceptibility of these cells to both apoptosis (Olichon et al., 2007) and oxidative stress (Zanna et al., 2008; Formichi et al., 2015), and when OPA1 is depleted by RNA interference there is reduced mitochondrial DNA content (Elachouri et al., 2011).

Our lab has previously reported a heterozygous mutant *Opa1* mouse, B6;C3-*Opa1*^{Q285STOP}, hereafter referred to as *BL/6-Opa1*$^{+/-}$ (Davies et al., 2007). The *Opa1* heterozygous nonsense mutation c.853C > T, located in exon 8 immediately before the central dynamin-GTPase, results in protein truncation and ca. 50% reduction in Opa1 protein expression in retina (Davies et al., 2007). This Opa1 deficiency affects retinal ganglion cells in an age-dependent manner (Williams et al., 2010). In mice over 12 months of age, mitochondria along the dendrites of ON-center retinal ganglion cells appear fragmented and lose cristae length, and neuronal dendrites recede and shorten (dendropathy) (Williams et al., 2010, 2012). At 15 months, PSD-95 immunostaining revealed reduced synaptic density in sublamina *b*, the locale where ON-center retinal ganglion cells receive their inputs (Williams et al., 2012). The dendropathy is sufficient to result in optic nerve degenerative changes visible on electron microscopy, and reduced visual acuity and retinal ganglion cell function, documented in *BL/6-Opa1*$^{+/-}$ mice by optokinetic testing and retinal electrophysiology (Davies et al., 2007; Barnard et al., 2011). In addition to retinal abnormalities, heart tissue from *BL/6-Opa1*$^{+/-}$ mice at 12 months showed decreased ATP levels and Complex I and IV deficiencies in mitochondria (Chen et al., 2012).

Idebenone is a synthetic benzoquinone and structurally very similar to ubiquinone, a key component in the mitochondrial respiratory chain (Gueven et al., 2015). Idebenone is soluble in oral preparations and sufficiently lipophilic to permeate cellular membranes (Erb et al., 2012), and is reduced via two-electron transfer to the hydroquinone form by NAD(P)H:quinone oxidoreductase-1 (NQO1, Haefeli et al., 2011). This reduction step is critical in its ability to transfer electrons to Complex III of the mitochondrial respiratory chain, and in turn maintain mitochondrial membrane potential and rescue ATP levels in tissue-cultured cells compromised with the Complex I inhibitor rotenone (Haefeli et al., 2011; Erb et al., 2012; Giorgio et al., 2012). Idebenone is known to inhibit lipid peroxidation and is a powerful antioxidant (Suno and Nagaoka, 1984; Erb et al., 2012). In a mouse model of Huntington's disease, idebenone delayed the development of cardiac hypertrophy (Seznec et al., 2004). However, idebenone can promote formation of superoxide radicals under certain conditions and its mode of action is incompletely understood (King et al., 2009).

Human clinical studies have shown high doses of idebenone are well tolerated, with only minor gastrointestinal complaints, and correlate with modest clinical score improvements in patients with Friedreich's ataxia and Leber's hereditary optic neuropathy (Di Prospero et al., 2007; Bodmer et al., 2009; Kutz et al., 2009; Carelli et al., 2011; Klopstock et al., 2011; Parkinson et al., 2013; Buyse et al., 2015). A small uncontrolled, open-label case series in seven dominant optic atrophy patients using idebenone at doses of between 270 mg and 1000 mg per day over one year found that two of the patients reported no subjective visual improvements, although the overall mean visual acuity from the cohort did improve and in four patients did so bilaterally (Barboni et al., 2013). A reduction in scotoma size and greater color discrimination and retinal nerve fiber layer thickness was evident, albeit disparate between individuals likely owing to patients recruited at different stages of disease, having varied mutations, ages, and idebenone dosages given (Barboni et al., 2013). Understandably, these clinical data are insufficient to justify the use of idebenone and further data are needed to underpin a full clinical trial of idebenone in human disease.

Our aim in this study, the first to use idebenone in an experimental mouse model of dominant optic atrophy, was to undertake a randomized, placebo-controlled trial in *BL/6-Opa1*$^{+/-}$ mice. Our trial design was chosen to mirror a potential trial of idebenone in human patients, in patients receiving treatment at or following clinical diagnosis. We treated *BL/6-Opa1*$^{+/-}$ mice from the time of the onset of retinal ganglion cell degeneration, and report on its effects and therapeutic potential.

EXPERIMENTAL PROCEDURES

Ethical statement

All mice were housed in a secure facility and maintained under constant temperature (22 °C) and humidity (45–65%) on a 12 h day/12 h night cycle, with access to water and solid food *ad libitum* (2014 Teklad Global 14% protein rodent maintenance diet) in accordance with the Animal (Scientific Procedures) Act 1986. One week prior to the start of the trial, mice were singly housed in large, adjacent cages with environmental enrichment. They were then kept singly housed throughout the days of the trial.

Idebenone preparations, dosing and trial design

Idebenone(6-(10-hydroxydecyl)-2,3-dimethoxy-5-methyl-1,4-benzoquinone), marketed as Raxone® in the treatment of Leber's hereditary optic neuropathy, was obtained through a material transfer agreement with Santhera Pharmaceuticals (Lot 080091) and prepared as a 20 mg/ml stock solution in 0.5% carboxymethycellulose salt (SIGMA) by overnight stirring at 4 °C. In line with other authors, we found mice would only eat idebenone-laced rations when it was mixed with sugar. Heitz et al. (2012) used 4% sucrose in regular chow (Heitz et al., 2012), however the mice in our colony did not accept this (even at 8% sucrose). Therefore it was necessary to mix idebenone with jelly. Hartley's Jelly® was melted and mixed with idebenone (135 g in a final volume of 190 ml), and food rations equivalent to 2000 mg per kg mice body weight were pipetted into weighboats and stored at −20 °C for 1 month (initial and third-week mouse weights were used to calculate

individual mouse dosages). Placebo rations comprised 135 g jelly mixed with only 0.5% carboxymethycellulose salt (to a final volume of 190 ml).

The trial included 119 mice (generation 5–7 on C57BL/6J background), with 63 wildtype (38 male and 25 female) and 56 *BL/6-Opa1*$^{+/-}$ mutant mice (25 male and 31 female) randomly assigned into four groups; wildtype and *BL/6-Opa1*$^{+/-}$ mice that received either idebenone or placebo rations. Mice were 12 to 14 months (365 to 420 days) old at the start of the 60-day protocol and dendropathy and cellular assessments (ATP and oxidative stress) were primary endpoints. A second cohort of mice were on average 11 months old at the start of the 42-day protocol for visual assessment and NQO1 analysis. Mice were supplied a single ration each day for 42 or 60 consecutive days, and the daily consumption of each ration was recorded. Mice were weighed 1 week before the start of the trial, and thereafter every week until completion. Non-fasting blood glucose concentration tests were performed with an Accu-Chek® kit from Roche between 10 a.m. and 2 p.m. with blood sampled from the heart chamber following sacrifice. Non-fasting blood glucose concentration from age-matched wildtype mice only fed standard chow was also taken. We processed mice in small groups (average $n = 6$) to remove bias arising as a result of tissue preparation time. The brain and liver were removed for molecular assays, and retinas were flat-mounted for retinal ganglion cell labeling.

Genotyping

DNA samples of ear tissue were immersed in 50 μl of 50 mM sodium hydroxide and heated to 95 °C for 10 min. Samples were then neutralized with 10 μl of 1 M TrisHCl pH 7.0, vortexed and spun. 1 μl was used as a template in a PCR reaction of 35 cycles with annealing temperature 59 °C with the following primers to detect the mutant allele; forward 5′-TCTCTTCATG TATCTGTGGTCTTTG-3′, and reverse 5′-TTACCCGTG GTAGGTGATCATA-3′.

Molecular assays

Sagittal quartered brain and liver tissue samples were snap frozen in liquid nitrogen and stored at −80 °C. Samples for lipid peroxidation studies were held under argon gas at −80 °C in a sealed glass bottle.

For the ATP assay, brain and liver samples were processed to extract ATP according to the manufacturer's instructions (Abcam, Cambridge, UK). Briefly, tissue was homogenized and then deproteinated in ice-cold 4 M perchloric acid. Following neutralization, samples were spun and the supernatant, containing ATP, collected. Assays were performed using a 96-well plate and absorbance read at 570 nm after 60 min incubation at room temperature. Readings were compared to ATP standards provided in the kit. Five microliter of the homogenate was tested separately in a BCA assay (SIGMA) to determine the amount of tissue protein used in the ATP assay.

Brain tissue samples for the thiobarbituric acid reactive species (TBARS) assay were homogenized in 1X butylated hydroxytoluene and lysis buffer (Abcam, Cambridge, UK). It was important to spin samples and carefully pipette supernatant free from cellular debris before and after an incubation of 95 °C for 1 h with thiobarbituric acid (reconstituted in glacial acetic acid). Readings were taken at 540 nm in a BioTek plate reader. Readings were compared to malondialdehyde standards provided with the kit. A sample of the homogenate was taken to determine protein concentration as above.

Protein carbonyl assay and western blotting

Protein from mouse liver samples were homogenized in RIPA lysis buffer containing protease inhibitor cocktail (Sigma–Aldrich) and 2% 2-mercaptoethanol (Sigma–Aldrich). Protein carbonyl groups were measured with the OxyBlot™ protein oxidation detection kit (Merck Millipore, Nottingham, UK) following the manufacturer's instructions. 20 μg of total protein was separated on a 10–12% SDS–PAGE gel and transferred to a nitrocellulose membrane (Biorad, Hemel Hempstead, UK). Protein samples were incubated with blocking buffer (1% (w/v) bovine serum albumen in PBS pH 7.2–7.4) for 1 h at room temperature. A rabbit anti-2, 4-dinitrophenylhydrazone antibody (1:150) was applied in blocking buffer for 1 h at room temperature. After washing in 0.05% Tween-20, a goat anti-rabbit horseradish peroxidase secondary antibody was used at 1:300 for 1 h at room temperature and blots developed using the enhanced chemiluminescence detection kit (Biological Industries, Lichfield, UK) and Pierce CL-Xposure™ Film (Thermo Scientific, Paisley, UK).

Western blotting was performed on 20 μg total protein and ran on 10–14% SDS–PAGE gels. Protein was extracted from individual mouse brain and liver samples, and from retina samples pooled from 4 mice. A mouse anti-OPA1 antibody (BD Biosciences), rabbit anti-NQO1 (Abcam, Cambridge, UK), and mouse anti-actin (SIGMA) were used at 1/1000 overnight at 4 °C to probe for OPA1, NQO1 and actin protein. Following four washes, rabbit anti-mouse and goat anti-rabbit horseradish peroxidase secondary antibodies (SIGMA) were used at 1/2000 and 1/2000, respectively, at room temperature for 2–4 h before being developed as above.

Bands from multiple western blots were quantified using ImageJ software and normalized to actin for relative values (as percent change relative to wildtype).

Visual function assessment

We followed the EMPReSS method (http://empress.har.mrc.ac.uk/) to record optokinetic responses. Three and six weeks from the start of feeding idebenone or placebo, mice were placed on a platform within a drum and allowed to habituate in the dark for 10 min. Thereafter, mice spent 5 min in light before testing began. We used a spectroradiometer to set the illuminance to 250 candela at the level of the platform. The drum was rotated clockwise for 1 min, and after a

30 s rest period, the drum was rotated counter-clockwise for 1 min. Mice activity was recorded using a video camera and later assessed for the optokinetic response. The inner surface of the drum was lined with black-and-white stripes set at 1 cm intervals (representing 2° or 0.25 cycles/deg of visual arc), and was the highest level of resolution *BL/6-Opa1*$^{+/-}$ mice could detect (Davies et al., 2007). Mice that are able to detect the moving grating will begin moving their head in the same direction and with the same speed as the drum before turning back. We counted the total number of these head turns for both clockwise and counter-clockwise directions, and the total time the mice actively spent tracking. These tests were repeated three times in total with 3 min of rest in the dark between each test. Each mouse was tested on three separate days to generate a large number of observations for reliable quantification. Video files were anonymized by assigning them six-digit numerical IDs and assessed by two independent researchers.

Immunohistochemistry

Ten micrometer cryosections of brain and liver tissue samples, and 12 μm sections of retina were thawed in PBS and then boiled in citrate buffer pH 6.0 for 30 min. Slides were cooled to room temperature, washed in PBS with 0.1% Tween-20 and 0.1% Triton-X100, and then blocked for 1–2 h at room temperature in 10% fetal bovine serum. 1/400 anti-NQO1 antibody was applied in 5% fetal bovine serum overnight at 4 °C, washed three times before 1/500 anti-rabbit Alexa secondary antibody was applied. Slides were incubated in 1/500 TO-PRO®-3 (Life Technologies, Paisley, UK) for 5 min before being washed in PBS and mounted in ProLong Gold under a #1 coverslip (Life Technologies, Paisley, UK) mountant.

Retinal cell labeling and morphometric analysis

Retinal ganglion cells were DiOlistically labeled using a Helios Gene Gun (Bio-Rad) and imaged with a confocal microscope Zeiss (LSM 510, ×20, 0.8 N.A lens) (Williams et al., 2010). Serial slices were captured at a resolution of 1024 × 1024 pixels and taken at 0.4 μm incremental steps.

Each retinal ganglion cell image stack was copied and then randomly assigned 6-digit identifiers generated from www.random.org. In this way retinal ganglion cells could be traced without bias by two operators blinded to their origin. The simple neurite tracer plugin for ImageJ was used to delineate the dendrites of retinal ganglion cells and resulted in a dendritic skeleton for each that mapped to their dendritic tree. All imaged retinal ganglion cells were verified with the presence of an axon. The depth to which dendrites ramify in the inner plexiform layer was used to determine ON- (0–60%) versus OFF- (60–100%) retinal ganglion cells (Coombs et al., 2006). Following tracing, each file was then decoded and assorted into bins for each condition and genotype for further analysis.

Sholl analysis is a widely used measure of the complexity of retinal ganglion cell dendritic architecture (Sholl, 1953), and has been used as a sensitive readout of the earliest physical evidence of retinal damage in glaucoma (El-Danaf and Huberman, 2015). In our study, intersections were counted across 10 μm concentric rings up to a range of 470 μm. A trapezoidal calculation method was used to measure the area under each Sholl curve. The total dendritic length was calculated as the sum of all the individual paths from the tracing skeleton. For the dendritic territory, a straight-sided polygon was traced around the terminal ends of dendrites and the resulting area calculated within ImageJ. Individual primary, secondary and tertiary dendrites were identified from their corresponding traced skeleton. The branching index was calculated as in (Garcia-Segura and Perez-Marquez, 2014). Instead of taking negative values as zero, we separated positive and negative data to reflect the overall increase or decrease in branching, respectively.

Retinal ganglion cells' eccentricities were measured using the stage controller stepper attached to the microscope (Zeiss). The location of the optic nerve head was manually aligned and set at 0.00 μm.

Statistics

Values are expressed as mean ± SEM. Statistical significance between groups was estimated by one sample, single-tailed Student's *t*-tests, with Bonferroni correction where necessary, and values of $\leqslant p = 0.05$ were considered significant. Power calculations were performed in R, and for the treatment arm a sample number of $n = 14$ was sufficient to give us a power of 0.8 for changes as small as 15% for most metrics. Two-step cluster analysis was performed in SPSS Statistics 22.

RESULTS

Idebenone administration in a mouse model of dominant optic atrophy

The logistics of the trial we conducted is summarized in Fig. 1A. There were three protocols based on a 21-day, 42-day and 60-day timeline to measure and assess various molecular, cellular and physiological effects as outlined. The analysis was based on per-protocol treatments, defined by a ⩾75% consumption of planned dose density achieved. For ⩾75% dose density, mice had to eat at least 90% of their ration for at least 75% of the time (i.e., 16 days out of 21, 32 days out of 42, and 45 days out of 60). Our per protocol strategy specified doses within tight parameters in all mice so that the outcome of all four arms of the trial could be compared. During the course of treatment, eleven mice did not achieve the planned minimum dose density (of these, nine were from the wildtype idebenone arm of the trial). Four mice died during the course of the trial. Therefore our analysis was conducted on a total of 104 mice (Fig. 1B).

In brain tissue samples from *BL/6-Opa1*$^{+/-}$ mice, expression levels of Opa1 protein were reduced by 33.02% (Cv 0.13, $p = 0.044$) (Fig. 1C, D), consistent

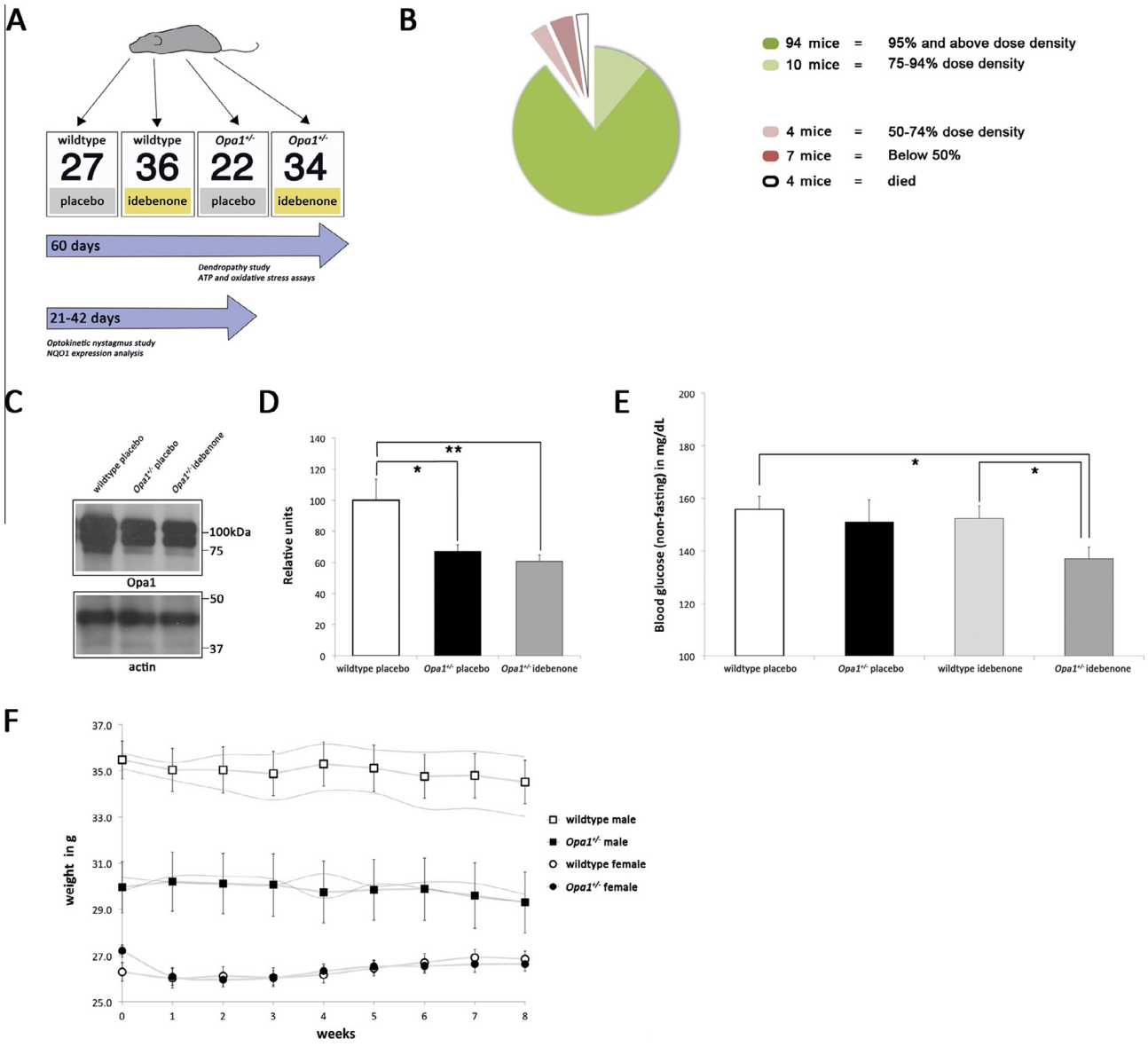

Fig. 1. Overview of placebo-controlled idebenone trial in *BL/6-Opa1*$^{+/-}$ mice. (A) Male and female mice at 12 to 14 months of age were randomly assorted into four groups: wildtype treated and untreated, and *BL/6-Opa1*$^{+/-}$ treated and untreated. Mice were fed idebenone per day for 21, 42 or 60 days. (B) Per protocol treatment chart showing the number of mice which ate their rations for the indicated completion of the trial. Fifteen mice were excluded from the trial. (C) Representative western blot for Opa1 protein (actin control) from brain tissue. (D), Densitometry of placebo-fed wildtype ($n = 6$) and *BL/6-Opa1*$^{+/-}$ mutant mice ($n = 4$), and from idebenone-fed *BL/6-Opa1*$^{+/-}$ mutant mice ($n = 6$). (E) Mean non-fasting blood glucose levels taken from wildtype and *BL/6-Opa1*$^{+/-}$ mice at time of death. (F) Weekly weight of surviving male mice (wildtype $n = 33$; *BL/6-Opa1*$^{+/-}$ $n = 16$), and female mice (wildtype $n = 18$; *BL/6-Opa1*$^{+/-}$ $n = 18$). Dashed lines above and below male plots show the difference in weight of mice that had either placebo or idebenone in their rations. Week 0 is weight before start of the trial.

with our previous findings and reports in other murine *Opa1*$^{+/-}$ models (Alavi et al., 2007; Davies et al., 2007; Sarzi et al., 2012). Opa1 protein levels did not change from baseline after idebenone treatment (Fig. 1D).

To assess if there were any effects from the diet administered, we measured weekly body weight and non-fasting blood glucose levels at the end of the testing period. Wildtype mice in the trial fed placebo rations had a mean non-fasting blood glucose level of 155.81 mg/dL (152.34 mg/dL for those wildtype mice fed idebenone-laced rations) and *BL/6-Opa1*$^{+/-}$ mice fed placebo rations had a mean non-fasting blood glucose level of 151.05 mg/dL (Fig. 1E). When compared to wildtype animals at 10 to 12 months of age fed only standard chow, which had a non-fasting mean blood glucose concentration of 159.3 mg/dL (data not shown), we found there was no significant effect incurred from the increased sugar in the diet. The mean non-fasting blood glucose concentration for *BL/6-Opa1*$^{+/-}$ mice fed idebenone was reduced to 136.92 mg/dL, and was significantly different from wildtype mice administered with idebenone ($p = 0.012$), or on placebo rations ($p = 0.004$) (Fig. 1E). No mouse had a blood glucose concentration in the range of 200–450 mg/dL, values

that are accepted as indicative of diabetes in mice used in diabetes research (Wu et al., 2001; Barber et al., 2005; Lee et al., 2006; Zhang et al., 2011). Additionally, across 8 weeks of the trial the weight of both male and female mice remained stable (Fig. 1F). Wildtype males were significantly heavier than their *BL/6-Opa1*$^{+/-}$ mutant littermates by 16.5% or 5.0 g (Fig. 1F, $p \leqslant 0.05$, Bonferonni correction). There were no statistically significant differences in weight between female wildtype and *BL/6-Opa1*$^{+/-}$ mutant littermates. Consumption of idebenone-laced rations over placebo produced only a small difference in weight between wildtype male mice (Fig. 1F), but not so *BL/6-Opa1*$^{+/-}$ mutants (Fig. 1F) or between female mice (data not shown).

Differences exist between male and female brain ATP levels in *BL/6-Opa1*$^{+/-}$ mice

All data on ATP levels came from the brains of the same mice whose retinal explants were used in the dendropathy study. The baseline level of ATP in brain tissues relative to total tissue protein in 14 to 16-month-old placebo-fed wildtype mice was 4.52 nmol/mg (95% CI 4.20 to 4.85, Cv 0.13; Fig. 2A), which is consistent with previous reports (Gkotsi et al., 2014). In male *BL/6-Opa1*$^{+/-}$ mutant brain tissue, baseline ATP levels were 5.41 nmol/mg (95% CI 4.41 to 6.41, Cv 0.15, $p = 0.051$). By contrast, in female *BL/6-Opa1*$^{+/-}$ mutant brain tissue we found a modest but significant reduction down to 3.93 nmol/mg (95% CI 3.55 to 4.40, Cv 0.12, $p = 0.042$) (as indicated in Fig. 2A). The difference in baseline ATP levels between male and female heterozygous brain tissue was statistically significant ($p = 0.002$).

We found that female *BL/6-Opa1*$^{+/-}$ mutant mice on a 60-day regimen of 2000 mg/kg per day of idebenone showed an increase in ATP levels to 4.50 nmol/mg (95% CI 4.04 to 4.96, Cv 0.13, $p = 0.035$; as indicated in Fig. 2A) as compared to untreated mice. Recovery of ATP levels in ß-islet cells could promote insulin release and be responsible for the reduced blood glucose levels seen in treated *BL/6-Opa1*$^{+/-}$ mice (Fig. 1E) (Zhang et al., 2011).

However, we planned our trial to analyze data from male and female mice inclusively, and overall we found that *BL/6-Opa1*$^{+/-}$ mutant mice fed on a 60-day regimen of 2000 mg/kg per day of idebenone showed no change in ATP levels as compared to untreated mice (Fig. 2A).

Idebenone-treated *BL/6-Opa1*$^{+/-}$ mice exhibit increased levels of protein carbonylation

We tested for products downstream of lipid peroxidation, such as malondialdehyde, using a traditional TBARS assay (Fig. 2B). However we did not find any significant differences between wildtype and *BL/6-Opa1*$^{+/-}$ mutant mice (Cv 0.48, $p = 0.108$), or for an effect of idebenone (Cv 0.22, $p = 0.127$). There was no change in lipid

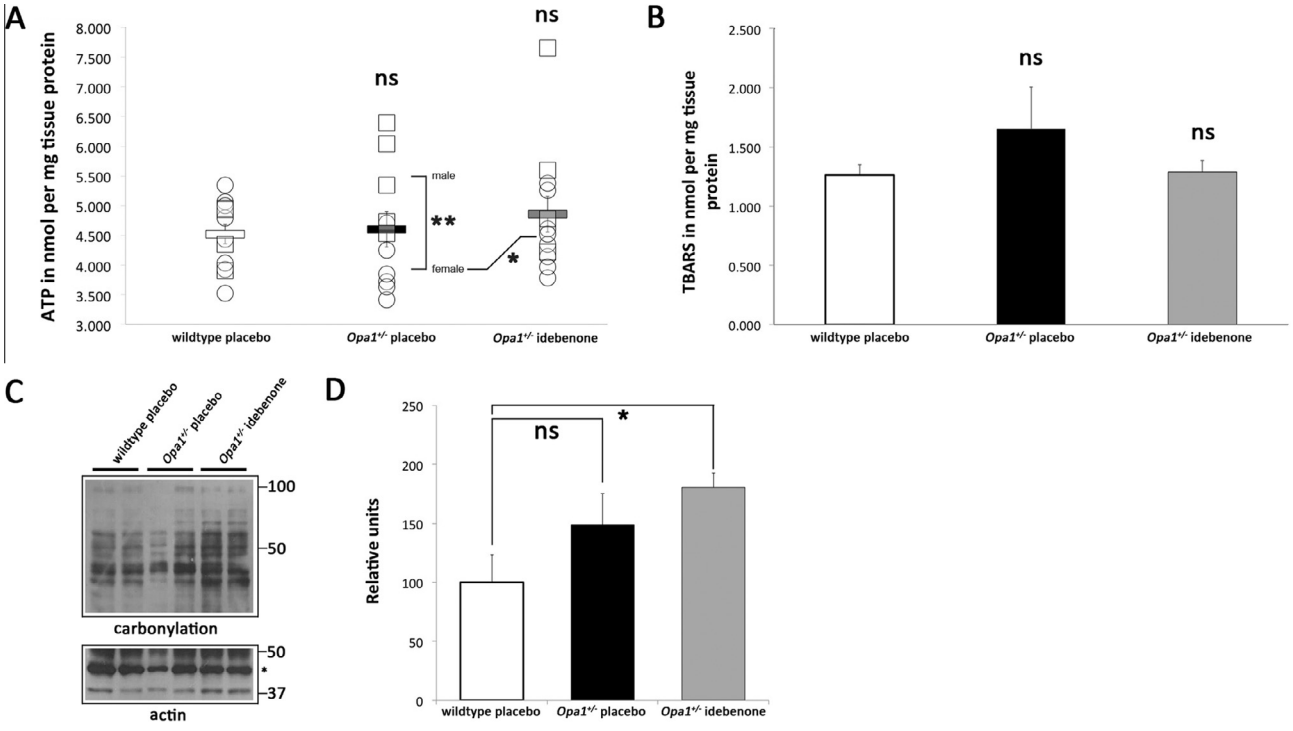

Fig. 2. Idebenone does not affect ATP levels in *BL/6-Opa1*$^{+/-}$ mice but does induce superoxide formation. (A) Brain samples from both male and female mice were assessed for ATP levels per mg tissue protein in placebo-fed wildtype ($n = 12$) and *BL/6-Opa1*$^{+/-}$ mice ($n = 11$), and idebenone-fed *BL/6-Opa1*$^{+/-}$ mice ($n = 12$). Absolute values are shown for males in squares and females in circles, horizontal bars represent mean ± SEM. Brackets show mean for male and female separately. (B), Brain samples were tested for lipid peroxidation derivatives in placebo-fed wildtype ($n = 8$) and *BL/6-Opa1*$^{+/-}$ mice ($n = 5$), or idebenone-fed *BL/6-Opa1*$^{+/-}$ mice ($n = 8$). (C), Representative western blot for protein carbonyl groups (actin control marked by asterisk) from liver tissue. (D) Densitometry of placebo-fed wildtype ($n = 4$) and *BL/6-Opa1*$^{+/-}$ mutant mice ($n = 3$), and idebenone-fed *BL/6-Opa1*$^{+/-}$ mutant mice ($n = 4$). $^{*}p < 0.05$, $^{**}p \leqslant 0.01$.

peroxidation reported in another *Opa1* mutant mouse line (Piquereau et al., 2012).

When we tested for protein carbonyl groups, formed as a result of increased oxidative stress, we found no significant differences between wildtype and *BL/6-Opa1*$^{+/-}$ mutant mice (Fig. 2C, D). However, in the presence of idebenone, treated *BL/6-Opa1*$^{+/-}$ mutant mice displayed a significant 80.35% increase in the levels of protein carbonylation (Cv 0.14, $p = 0.011$) (Fig. 2D).

Idebenone does not significantly reduce the extent of retinal ganglion cell dendropathy in *BL/6-Opa1*$^{+/-}$ mice

Labeled retinal ganglion cells from mice in all four arms of the trial were analyzed and included both ON-center (Fig. 3A–L) and OFF-center types (Fig. 4). These cells were sampled from various eccentricities across the retina to provide an accurate reflection of overall health status (Fig. 3Q). As expected from previous work (Williams et al., 2010), ON-center retinal ganglion cells from *BL/6-Opa1*$^{+/-}$ mice showed a significant deterioration of 51.91% in dendritic complexity (Cv 0.49, $p = 0.007$, Fig. 3M, P), total dendritic length was 2.30 mm shorter (Cv 0.51, $p = 0.017$; Fig. 3R), and dendritic territory was reduced by 2.46×10^4 μm^2 (Cv 0.54, $p = 0.008$; Fig. 3S) when compared to wildtype. The branching index analysis (BI) found the positive BI fell by 0.70×10^3 (Cv 0.65, $p = 0.041$) and the negative component was reduced by 2.49×10^3 (Cv 0.60, $p = 0.008$) (Fig. 3T), suggesting a more severe dendritic reduction in secondary and tertiary branches of *BL/6-Opa1*$^{+/-}$ mutant retinal ganglion cells. We found that secondary branches in *BL/6-Opa1*$^{+/-}$ ON-center retinal ganglion cells were reduced more than primary and tertiary branches in those cells, and by 0.91 mm compared to wildtype retinal ganglion cells (Cv 0.59, $p = 0.009$; Fig. 3U).

In *BL/6-Opa1*$^{+/-}$ mutant mice treated with idebenone, we saw an upward and rightward shift in the Sholl profile (Fig. 3N), with 22.35% recovery in the area under the curve compared to untreated *BL/6-Opa1*$^{+/-}$ mice (denoted by *i* in Fig. 3P). However, this result was not statistically significant (Cv 0.97, $p = 0.157$). There was improved total dendritic length, being 1.14 mm longer than it otherwise would have been (Fig. 3R), and dendritic territory was greater by 2.22×10^4 μm^2 (Fig. 3S). The branching index was higher (positive by 0.55×10^3, negative by 1.42×10^3, Fig. 3T). However this was not statistically significant for total dendritic length ($p = 0.159$) or branching index (positive $p = 0.133$, negative $p = 0.115$), although for average dendritic territory there was a trend toward improvement ($p = 0.074$) (see below).

Idebenone may offer some protection to secondary dendritic branches and dendritic territory in *BL/6-Opa1*$^{+/-}$ mutant mice

When we identified primary, secondary and tertiary dendrites and plotted their values separately we found a small beneficial effect of idebenone (Fig. 3U). In ON-center retinal ganglion cells from idebenone-treated *BL/6-Opa1*$^{+/-}$ mice, the accumulative dendritic length for primary, secondary and tertiary dendrites was increased over untreated mice by 0.31 mm, 0.49 mm, and 0.33 mm, respectively. For secondary dendrites this was equivalent to 53.89% of the actual loss of secondary dendritic length in *BL/6-Opa1*$^{+/-}$ retinal ganglion cells (Cv 0.78, $p = 0.052$). While these data do not reach significance, they suggest a potential therapeutic effect of idebenone. We also noted that the secondary branch length (1.10 mm) and dendritic territory (4.61×10^4 μm^2, Fig. 3S) of retinal ganglion cells from idebenone treated *BL/6-Opa1*$^{+/-}$ mice have similar values to those found in wildtype mice (1.52 mm and 4.85×10^4 μm^2, respectively). Comparing untreated wildtype and treated *BL/6-Opa1*$^{+/-}$ retinal ganglion cells as an indicator of therapeutic benefit, we see no statistically significant differences in dendritic territory ($p = 0.129$) (Fig. 3S) or secondary dendritic length ($p = 0.139$) (Fig. 3U), suggesting that idebenone may have a protective effect, sufficient to allow the idebenone-treated *BL/6-Opa1*$^{+/-}$ retinal ganglion cells to retain these aspects of their dendritic architecture.

Idebenone has significant deleterious effects on wildtype retinal ganglion cells and visual function

The Sholl profiles for labeled ON- and OFF-center retinal ganglion cells from wildtype mice given idebenone showed a significant fall of 38.49% (Cv 0.57, $p = 0.030$) and 47.37% in area under the curve (Cv 0.57, $p = 0.029$), respectively (Figs. 3O, P, 4C, D). This was also reflected in OFF-center wildtype retinal ganglion cells by calculating the branching index. Idebenone caused the positive BI to fall by 1.37×10^3 (Cv 0.73, $p = 0.003$) and the negative BI to fall by 2.99×10^3 (Cv 0.65, $p = 0.009$) (Fig. 4E). We also saw a reduction in the total dendritic length for ON- and OFF-center retina ganglion cells, with deterioration of 1.61 mm (Cv 0.58, $p = 0.054$) and 2.40 mm (Cv 0.55, $p = 0.025$), respectively (Fig. 3R, 4F). In addition, idebenone caused a reduction in the dendritic territory (down by 1.87×10^4 μm^2, Cv 0.65, $p = 0.029$) in ON-center retinal ganglion cells (Fig. 3S).

This detrimental effect of idebenone appears to be reflected in the visual function as assessed by optokinetic response. In wildtype mice fed idebenone, we saw no significant reduction in total tracking time but the total number of head turns was significantly reduced to 9.2 ± 0.7 compared to placebo wildtype mice ($p = 0.007$, Fig. 5B).

In an early phase of the disease idebenone restored vision in *BL/6-Opa1*$^{+/-}$ mice but this effect was not sustained

We determined visual function in mice following an optokinetic response protocol by assessing the head turning reflex, in which mice will turn their head in the direction of a moving grating and track for a length of time (Fig. 5A). On average placebo-fed wildtype mice

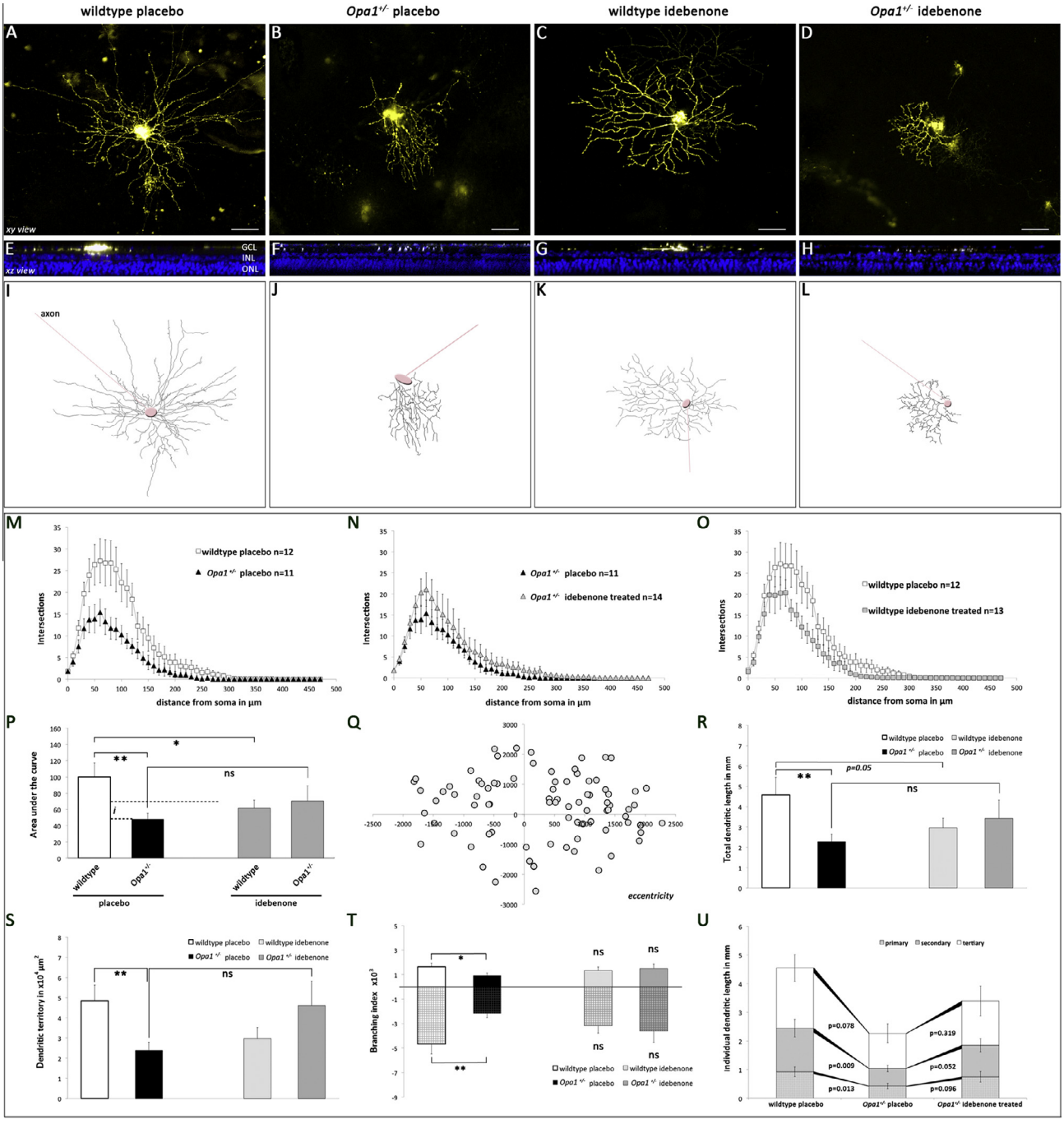

Fig. 3. Idebenone fails to significantly alter dendritic complexity in *BL/6-Opa1*$^{+/-}$ ON-center retinal ganglion cells. (A–D), representative retinal ganglion cell labeled with DiI (shown in yellow) from (A) wildtype mice, (B) *BL/6-Opa1*$^{+/-}$ mice, (C) wildtype mice given idebenone (D) *BL/6-Opa1*$^{+/-}$ mice treated with idebenone. (E–H), *xz* view of stack, counterstained with TO-PRO®-3 to show retinal layers. (I–L), Compiled *z*-stack images of traced retinal ganglion cell dendrites. Circles show cell body of retinal ganglion cell, with solid line indicating location of axon. Scale bar = 50 μm. (M–O) Sholl profile showing dendritic complexity for ON-center retinal ganglion cells. (M) comparison between wildtype (n = 12 from 7 mice) and *BL/6-Opa1*$^{+/-}$ (n = 11 from 5 mice) cells from mice given placebo. (N) comparison between *BL/6-Opa1*$^{+/-}$ cells from mice given placebo or treated with idebenone (n = 14 from 6 mice). (O) Comparison of cells from wildtype mice given placebo or administered with idebenone (n = 13 from 6 mice). (P) The area under the curve for each Sholl plot is shown as percent change relative to wildtype. Dashed lines show the difference in area between *BL/6-Opa1*$^{+/-}$ retinal ganglion cells and those from *BL/6-Opa1*$^{+/-}$ mice treated with idebenone. ***i*** marks potential recovery caused by idebenone. (Q) The eccentricity of all retinal ganglion cells analyzed in the study. (R) The total dendritic length from ON-center retinal ganglion cells is shown for each condition, and likewise for, (S) the dendritic territory and (T) the branching index. (U) The dendritic lengths of primary (those dendrites that originate at soma), secondary (originate from primary dendrites) and tertiary dendrites are shown. $^{*}p < 0.05$, $^{**}p \leqslant 0.01$. ns = not significant i.e., $p > 0.05$. GLC, ganglion cell layer; INL, inner nuclear layer; ONL, outer nuclear layer. (For interpretation of the references to colour in this figure legend, the reader is referred to the web version of this article.)

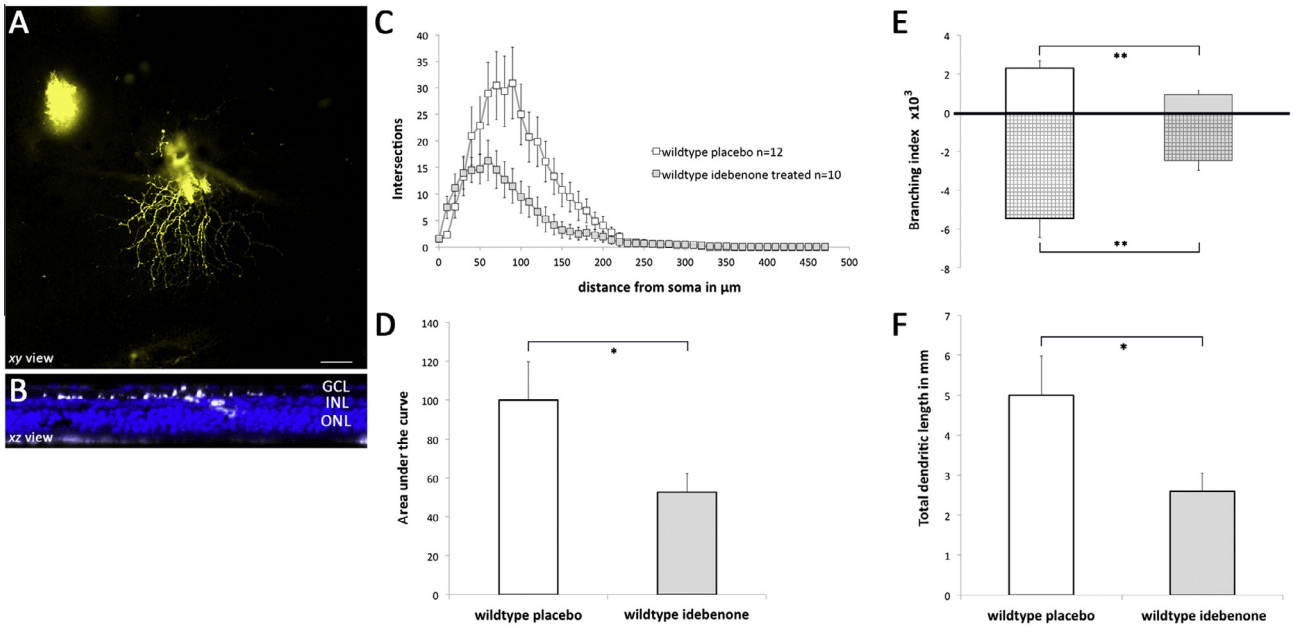

Fig. 4. Idebenone has deleterious effects for wildtype OFF-center retinal ganglion cells. (A) A representative OFF-center retinal ganglion cell with DiI demarcating dendrites and soma. Scale bar = 50 μm. (B) *xz* view across the retina. (C) Sholl plot comparison between OFF-center retinal ganglion cells taken from placebo-fed wildtype mice (n = 12 from 6 mice) and idebenone-fed wildtype mice (n = 10 from 5 mice). (D) The area under the curve for each Sholl plot is shown as percent change relative to wildtype. (E) Separated values for positive and negative branching index. (F) Measurements of the sum total of dendritic length for each retinal ganglion cell. $^{*}p < 0.05$, $^{**}p \leqslant 0.01$.

performed 12.1 ± 0.9 head turns (Fig. 5B) for a total 33.3 ± 2.3 s (Fig. 5C) during the testing period (both clockwise and counter-clockwise directions). In placebo-fed *BL/6-Opa1*$^{+/-}$ mice there were fewer turns (7.8 ± 0.6, $p < 0.01$) and a reduced tracking time (25.7 ± 1.9 s, $p = 0.007$), which is comparable to our previous published report (Davies et al., 2007). Feeding *BL/6-Opa1*$^{+/-}$ mice idebenone did not appreciably affect the number of head turns (8.1 ± 0.6) but did show an apparent improvement in total tracking time (30.1 ± 2.5 s). This result did not reach significance.

However, when we looked at the tracking time from 3 weeks after the start of the trial, mice did show a substantial improvement in tracking time (by 12.2 ± 3.2 s, $p = 0.003$; dashed upper bar in Fig. 5C) and an increase in the number of head turns (by 1.75 ± 0.8, $p = 0.048$; dashed bar in Fig. 5B). In contrast, by 6 weeks after the start of the trial, the vision in *BL/6-Opa1*$^{+/-}$ mice had deteriorated to a total of 20.1 ± 2.9 s (dashed lower bar in Fig. 5C), similar to pre-treatment levels. The difference in tracking time between 3 weeks and 6 weeks was very significant ($p < 0.01$).

The expression of NQO1 protein in response to idebenone is variable and tissue-specific

We performed expression analysis on brain, retina and liver tissue samples from our 42-day protocol of idebenone administration. In brain, both wildtype and *BL/6-Opa1*$^{+/-}$ mice have some cells that express NQO1 protein in the cytoplasm (Fig. 6A), and in retina NQO1 protein is found within the ganglion cell layer as well as the inner segment of the photoreceptive layer (Fig. 6D). In *BL/6-Opa1*$^{+/-}$ mice liver, NQO1 protein is robustly expressed in most parenchymal cells (Fig. 6G). Western blotting from mice fed idebenone or placebo revealed that NQO1 protein is dynamically expressed in different tissues. In *BL/6-Opa1*$^{+/-}$ brain tissue, NQO1 protein is expressed 69.5% less than in wildtype brain ($p = 0.002$, Fig. 6B, C), and while idebenone induced a higher expression of NQO1 protein in wildtype brain (by 24.2%, $p = 0.027$), it did not do so in *BL/6-Opa1*$^{+/-}$ mice fed idebenone (Fig. 6C). Idebenone substantially induced NQO1 protein expression in wildtype liver tissue as well (by 719.7%, $p = 0.0003$, Fig. 6H, I). In contrast to brain, *BL/6-Opa1*$^{+/-}$ liver showed higher NQO1 expression (by 776.1%, $p = 0.037$, Fig. 6I). In the retina there were no significant differences in the level of NQO1 protein, either due to genotype or treatment condition (Fig. 6E, F).

DISCUSSION

We present data on the first trial of idebenone in a mouse model of dominant optic atrophy. Our mutant mouse model shows very clear morphometric abnormalities in ON-center retinal ganglion cell dendrites that prove invaluable indices to accurately quantify the effect of treatment with idebenone. The importance of dendritic morphology as a structural marker underlying vision is highlighted by a recent study that has used these metrics to assess the earliest indicators of glaucoma (El-Danaf and Huberman, 2015). Assessment of dendritic morphology has also been used to measure the effectiveness of other therapeutic agents following optic nerve crush (Lindsey et al., 2015a,b). In fact, perturbations to functional receptive fields and electrophysiology readings

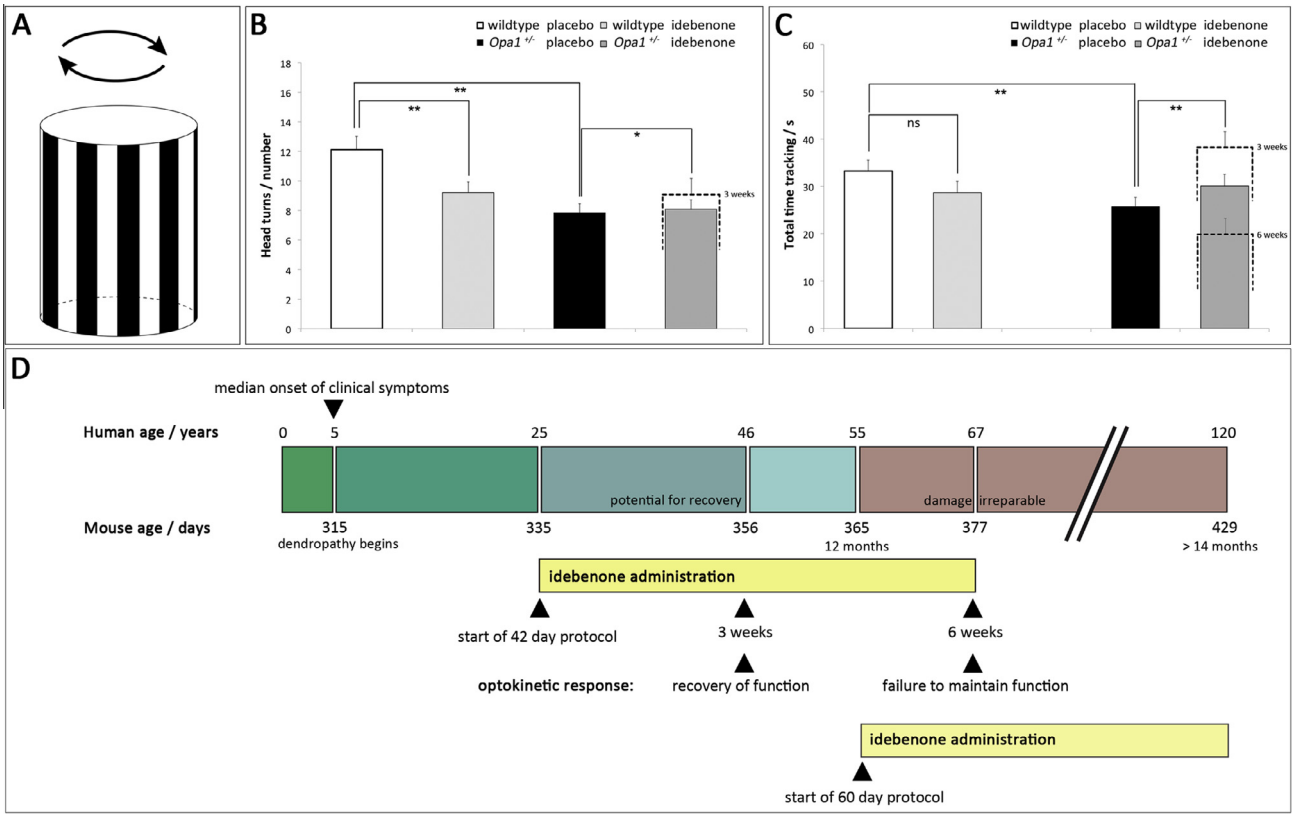

Fig. 5. Visual assessment of mice shows a temporary improvement in vision after short idebenone exposure. (A) Drum was lined with 1 cm black-and-white stripes and rotated clockwise (shown here) or counter-clockwise. (B) The number of head turns for both directions during the 42-day protocol are shown. (C) The total time spent tracking in both directions during the 42-day protocol are shown. Inset dashed lines show the respective values obtained mid-way through the protocol and at its end. (D) Schematic relating the age between human patients and our mouse model with respect to retinal disease (http://rubinlab.bgu.ac.il/mouseAPK/H2M/index.html). We used the search term "retinal degeneration," which gave a Pearson correlation of 0.50. The start point of our trial and key times when mice were assessed are shown. 120 human years is the limit of the database, and therefore the 14 to 16 months protocol is not shown. $^{**}p \leqslant 0.01$. ns = not significant i.e., $p > 0.05$.

of some, but not all, retinal ganglion cell types have been found to occur concomitantly with structural changes in dendrites, specifically the dendritic length, dendritic territory and Sholl profile (Della Santina et al., 2013). Our results suggest that idebenone has a small measurable effect in protecting certain retinal ganglion cell dendritic parameters, specifically the length of the secondary branches and dendritic territory. However, overall there is little statistically significant benefit on retinal ganglion cell dendropathy, casting doubt on the potential of idebenone to restore normal function after the onset of disease in our mouse model.

The route of administration could have hindered the therapeutic effect of idebenone, and questions arise around the appropriate dose and how to achieve it. Oral administration of idebenone invariably results in rapid first-pass metabolism by the liver and severely reduced and short-lived plasma concentrations (Bodmer et al., 2009; Kutz et al., 2009; Becker et al., 2010). In mice, a single dose of idebenone at 60 mg/kg delivered by gavage resulted in a maximum concentration peak of 9 ng/ml (26.6 nM) and 37.4 ng/ml (110.5 nM) in the vitreous and aqueous humor, respectively, but falling to levels below the limit of quantification after just 30 min and 120 min, respectively (Heitz et al., 2012). Many experiments conducted on *in vitro* cultured cells use idebenone concentrations at 10,000 nM (even to 100,000 nM in some cases), and it is where many authors have apparently demonstrated the effectiveness of idebenone in restoring various cellular functions (Suno and Nagaoka, 1984; Heitz et al., 2012; Fiebiger et al., 2013). The question of whether we should have opted for higher doses of idebenone to increase concentration at target sites is an important one, considering values in aqueous humor were shown to rise proportionally in response to increasing the amount of idebenone (Heitz et al., 2012). However it is clear that idebenone can produce measurable effects at even lower concentrations in tissue-cultured cells. Heitz et al. have shown that 10 nM was the minimum concentration of idebenone required to rescue rotenone-compromised RGC-5 cells (Heitz et al., 2012). Importantly these values were also obtained in mouse vitreous and aqueous humor following 21 days of idebenone given as a food supplement at a dosage of 2000 mg/kg per day (Heitz et al., 2012). Our choice of a 2000 mg/kg per day dosage is therefore supported by the literature and likely to be more than sufficient to produce biologically significant effects.

In addition, expression and activity of NQO1 are important prerequisites for any treatment plan involving

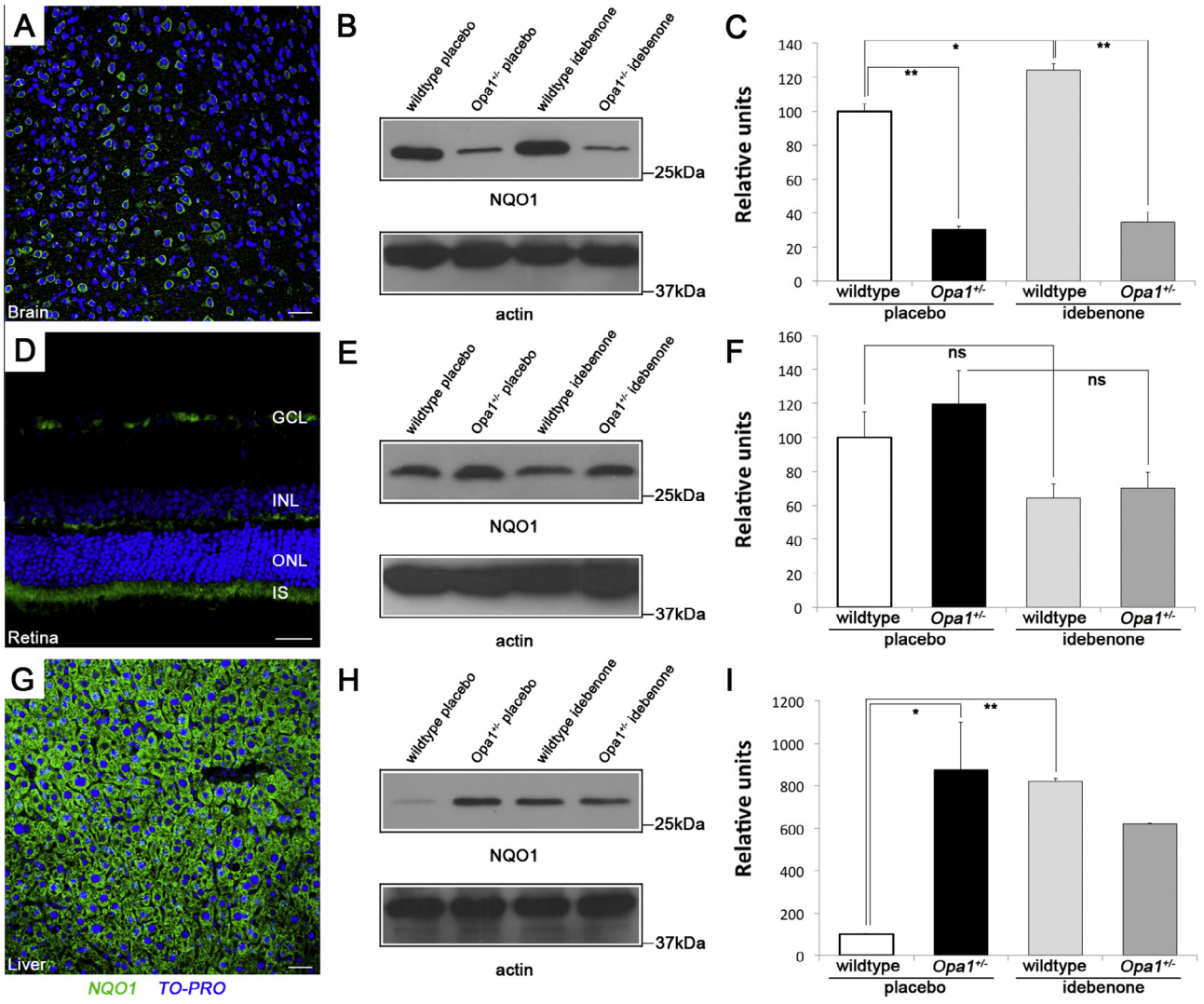

Fig. 6. Expression level of NQO1 protein is tissue-specific and determines the extent of idebenone's therapeutic effect. (A, D, G) Immunohistochemistry showing tissue-specific NQO1 expression in brain, retina and liver. Scale bar = 50 μm. (B ,E, H) Representative western blots for NQO1 (actin as control) in brain, retina and liver tissue. (C) Densitometry of brain samples from placebo-fed wildtype ($n = 2$) and *BL/6-Opa1*$^{+/-}$ mutant mice ($n = 2$), and idebenone-fed *BL/6-Opa1*$^{+/-}$ mutant mice ($n = 2$). F), Densitometry of pooled retina samples from placebo-fed wildtype ($n = 4$) and *BL/6-Opa1*$^{+/-}$ mutant mice ($n = 4$), and idebenone-fed *BL/6-Opa1*$^{+/-}$ mutant mice ($n = 4$). (I) Densitometry of liver samples from placebo-fed wildtype ($n = 2$) and *BL/6-Opa1*$^{+/-}$ mutant mice ($n = 2$), and idebenone-fed *BL/6-Opa1*$^{+/-}$ mutant mice ($n = 2$). $^{*}p < 0.05$. $^{**}p \leqslant 0.01$. ns = not significant i.e., $p > 0.05$. GLC, ganglion cell layer; INL, inner nuclear layer; IS, inner segment; ONL, outer nuclear layer.

idebenone. We have found a tissue-specific variability in NQO1 protein expression in response to idebenone, as well as in the expression of NQO1 protein in *BL/6-Opa1*$^{+/-}$ mice. The levels of NQO1 protein were reduced in brain samples from *BL/6-Opa1*$^{+/-}$ mice, and this would necessarily limit the potential benefit of idebenone in this tissue. Others have discussed implications of a combinatorial therapy whereby *NQO1* expression in target tissues could be upregulated using compounds that promote its transcription via Nrf2 (Jaber and Polster, 2015). This would increase availability of NQO1 in neurons and we would expect it to enhance idebenone's electron carrier role.

In retina, NQO1 protein levels remain unchanged between wildtype and *BL/6-Opa1*$^{+/-}$ mice, and retinal ganglion cells expressed NQO1 as shown previously (Heitz et al., 2012). Therefore in our trial of idebenone in a mouse model of dominant optic atrophy, the reported actions of idebenone were not a limiting factor.

Our cellular analysis uncovered a negative effect of idebenone on retinal ganglion cell health in wildtype mice without a mitochondrial deficit. This was unexpected, since idebenone has been shown to prevent cultured neuronal cells from glutamate-induced excitotoxicity and amyloid ß-peptide-induced neurotoxicity (Hirai et al., 1998; Fiebiger et al., 2013), and can protect male Sprague-Dawley rats from kainic acid-induced intrastriatal neuronal degeneration *in vivo*(Miyamoto and Coyle, 1990). Nonetheless, both ON- and OFF-center retinal ganglion cells from wildtype mice treated with idebenone displayed a profound deterioration in their dendritic morphology.

This accumulative deleterious effect could be due to oxidative stress. Interestingly, idebenone is sufficient to indirectly induce the expression of NQO1 in wildtype

liver cells, suggesting that the presence of idebenone caused increased cellular stress. NQO1 is induced in the liver via the Nrf2 transcription factor as part of an antioxidant defense mechanism (Jaber and Polster, 2015; Cheng et al., 2015).

At high concentrations idebenone is known to inhibit Complex I activity (Esposti et al., 1996), and even cause the opening of the permeability transition pore complex (Walter et al., 2000). There are inhibitory effects of non-reduced idebenone on ATP synthesis and oxygen consumption rate (Giorgio et al., 2012). Idebenone can also bind to the hydrophobic quinone-binding site of Complex I and promote superoxide formation (King et al., 2009). These are all potential mechanisms for how idebenone could prove detrimental in treated mice, sufficient to reverse any initial, positive recovery. Recently, idebenone has been shown to inhibit activity of a calcium-activated chloride channel (Seo et al., 2015), which is expressed in axon terminals of bipolar cells (Jeon et al., 2013). In a human prostate cancer cell line and a cystic fibrosis pancreatic line, this inhibitory function resulted in cell death (Seo et al., 2015). If idebenone caused apoptosis in retinal neurons in a similar manner, this could have serious repercussions for those retinal ganglion cells that receive input from bipolar axons. Thus it may be that the exact dosage of idebenone is critical.

In order to evaluate whether the dendropathy seen in wildtype mice results in a functional effect on vision we assessed visual function by the optokinetic response (Davies et al., 2007). As expected we were able to confirm that *BL/6-Opa1*$^{+/-}$mutant mice displayed reduced visual function. The dendropathy see in OFF-center retinal ganglion cells from wildtype mice treated with idebenone was significant. The number of head turns documented in wildtype idebenone mice was statistically reduced as compared to wildtype placebo mice, although when assessing total time spent tracking this significance was lost, suggesting that the effect on visual function may be borderline.

Nonetheless, our study highlights a possible risk of using idebenone to treat patients with a misdiagnosis of mitochondrial optic neuropathy (e.g., dominant optic atrophy without *OPA1* mutation), or in treating patients with preclinical or subclinical disease. This potential for visual toxicity in unaffected eyes suggests caution will be needed until it can be shown that this does not result in or hasten visual loss.

In addition, we show differences between the genders of *BL/6-Opa1*$^{+/-}$ mice that will need to be considered in planning future studies in mice or man. This difference became evident when we looked at ATP levels in mutant brain tissue. While it could be argued that this finding is not clinically important, as there are no clear gender differences in morbidity for patients with dominant optic atrophy, this strongly suggests that future studies will need to stratify treatments by the gender of subjects.

Based on the findings of our dendropathy study, we measured visual function mid-way through the trial and at the end, in order to assess the time course of any potential effect of idebenone. We discovered after a short duration of idebenone treatment an improvement in the vision of *BL/6-Opa1*$^{+/-}$ mice, but this positive effect was reduced to pre-treatment levels in a short span of three weeks. This runs counter to the reported findings in Friedreich's ataxia, where a longer duration is associated with improved clinical scores (Parkinson et al., 2013).

It is well established that mouse life-span and aging is not linearly correlated to human life-span. The age-phenome knowledge database (http://rubinlab.bgu.ac.il/mouseAPK/H2M/index.html) models the relationship between mouse and human age based on specific disease classes (Geifman and Rubin, 2013). When we correlate the human age to the equivalent age of mice at the start of our trial, we noted that we began the 60-day protocol at the equivalent human age of 55 years old, and the 42-day protocol at a human age of 25 years old. Therefore the age at which medication is administered may be critical to treatment effect in patients. In the 42-day protocol, the administration of idebenone at a younger age may have contributed to apparent improvement in visual function. This fits well with the time-limited effects modeled in neurodegenerative disease progression (Porciatti and Ventura, 2012). From the age phenome theoretical model it is suggested that the 60-day administration of idebenone is hypothetically equivalent to more than 65 years of human life, thereby suggesting that we did administer the drug for an appropriately long period of time.

Idebenone is currently authorized in the EU as a treatment option for the mitochondrial optic neuropathy, Leber's hereditary optic neuropathy, which results from mitochondrial DNA mutations in Complex I genes (Yu-Wai-Man et al., 2014). The ability of idebenone to restore mitochondrial function under Complex I deficiency has been demonstrated in mice (Heitz et al., 2012). However, the aberrant mitochondrial effects that result from *OPA1* mutations are more varied than in Leber's hereditary optic neuropathy, with alternative roles for OPA1 including the regulation of thermogenesis and ß-oxidation (Quiros et al., 2012), the mediation of cell apoptosis through inhibiting cytochrome c release (Varanita et al., 2015), and in the response to cell starvation (Patten et al., 2014). These differences in pathophysiology may explain why idebenone is not equally effective in both disorders.

In summary, we have carried out a randomized placebo-controlled trial of idebenone in a mouse model of dominant optic atrophy. We have found some indication of therapeutic improvement with idebenone fed to mice at 2000 mg/kg per day from 11 months (335 days) of age. Initially, we found that a functional assessment of vision revealed a large improvement in visual acuity. After six weeks of treatment, visual acuity decreased to pre-treatment levels. Starting idebenone treatment at 12–14 months of age for 60 days showed only a slight indication of benefit, with the secondary dendritic length and dendritic territory in *BL/6-Opa1*$^{+/-}$mutant ON-center retinal ganglion cells being greater following idebenone administration. Overall however, idebenone did not alter the course of the retinal ganglion cell dendropathy.

In OFF-center retinal ganglion cells from wildtype retina, idebenone caused a severe reduction in retinal ganglion cell morphometric parameters, and this was mirrored by a reduced number of head turns in the optokinetic response functional visual assessment. Therefore, although idebenone may be a therapeutic option in the treatment of some mitochondrial optic neuropathies, our data suggest it should be used with caution in individuals where there is no mitochondrial dysfunction.

Acknowledgments—We thank Rhys Perry, Helen Read and Jean Rodgers for animal husbandry, and, Orosia Asby, Nuri Gueven, James Morgan, Malgorzata Rozanowska, Veronica Walker and Pete Williams for advice. We are grateful to Nick White for assistance with microscopy. Thanks to Kathy Beirne, Paul Cornes, Sally Hayes, James Morgan and Rob Young for critical reading of the manuscript. Idebenone was obtained through a Material Transfer Agreement with Santhera Pharmaceuticals.

This work was funded in part by the National Eye Research Centre (SCIAD 033) and by the University of Cardiff.
The authors declare no conflict of interests.

REFERENCES

Agier V, Oliviero P, Laine J, L'Hermitte-Stead C, Girard S, Fillaut S, Jardel C, Bouillaud F, Bulteau AL, Lombes A (2012) Defective mitochondrial fusion, altered respiratory function, and distorted cristae structure in skin fibroblasts with heterozygous OPA1 mutations. Biochim Biophys Acta 1822:1570–1580.

Alavi MV, Bette S, Schimpf S, Schuettauf F, Schraermeyer U, Wehrl HF, Ruttiger L, Beck SC, Tonagel F, Pichler BJ, Knipper M, Peters T, Laufs J, Wissinger B (2007) A splice site mutation in the murine Opa1 gene features pathology of autosomal dominant optic atrophy. Brain 130:1029–1042.

Alavi MV, Fuhrmann N (2013) Dominant optic atrophy, OPA1, and mitochondrial quality control: understanding mitochondrial network dynamics. Mol Neurodegener 8:32.

Alexander C, Votruba M, Pesch UE, Thiselton DL, Mayer S, Moore A, Rodriguez M, Kellner U, Leo-Kottler B, Auburger G, Bhattacharya SS, Wissinger B (2000) OPA1, encoding a dynamin-related GTPase, is mutated in autosomal dominant optic atrophy linked to chromosome 3q28. Nat Genet 26:211–215.

Barber AJ, Antonetti DA, Kern TS, Reiter CE, Soans RS, Krady JK, Levison SW, Gardner TW, Bronson SK (2005) The Ins2Akita mouse as a model of early retinal complications in diabetes. Invest Ophthalmol Vis Sci 46:2210–2218.

Barboni P, Valentino ML, La Morgia C, Carbonelli M, Savini G, De Negri A, Simonelli F, Sadun F, Caporali L, Maresca A, Liguori R, Baruzzi A, Zeviani M, Carelli V (2013) Idebenone treatment in patients with OPA1-mutant dominant optic atrophy. Brain 136: e231.

Barnard AR, Charbel Issa P, Perganta G, Williams PA, Davies VJ, Sekaran S, Votruba M, MacLaren RE (2011) Specific deficits in visual electrophysiology in a mouse model of dominant optic atrophy. Exp Eye Res 93:771–777.

Becker C, Bray-French K, Drewe J (2010) Pharmacokinetic evaluation of idebenone. Expert Opin Drug Metab Toxicol 6:1437–1444.

Bodmer M, Vankan P, Dreier M, Kutz KW, Drewe J (2009) Pharmacokinetics and metabolism of idebenone in healthy male subjects. Eur J Clin Pharmacol 65:493–501.

Buyse GM, Voit T, Schara U, Straathof CS, D'Angelo MG, Bernert G, Cuisset JM, Finkel RS, Goemans N, McDonald CM, Rummey C, Meier T, Group DS (2015) Efficacy of idebenone on respiratory function in patients with Duchenne muscular dystrophy not using glucocorticoids (DELOS): a double-blind randomised placebo-controlled phase 3 trial. Lancet 385:1748–1757.

Carelli V, La Morgia C, Valentino ML, Rizzo G, Carbonelli M, De Negri AM, Sadun F, Carta A, Guerriero S, Simonelli F, Sadun AA, Aggarwal D, Liguori R, Avoni P, Baruzzi A, Zeviani M, Montagna P, Barboni P (2011) Idebenone treatment in Leber's hereditary optic neuropathy. Brain 134:e188.

Chao de la Barca JM, Prunier-Mirebeau D, Amati-Bonneau P, Ferre M, Sarzi E, Bris C, Leruez S, Chevrollier A, Desquiret-Dumas V, Gueguen N, Verny C, Hamel C, Milea D, Procaccio V, Bonneau D, Lenaers G, Reynier P (2015) OPA1-related disorders: diversity of clinical expression, modes of inheritance and pathophysiology. Neurobiol Dis.

Chen L, Liu T, Tran A, Lu X, Tomilov AA, Davies V, Cortopassi G, Chiamvimonvat N, Bers DM, Votruba M, Knowlton AA (2012) OPA1 mutation and late-onset cardiomyopathy: mitochondrial dysfunction and mtDNA instability. J Am Heart Assoc 1: e003012.

Cheng ML, Lu YF, Chen H, Shen ZY, Liu J (2015) Liver expression of Nrf2-related genes in different liver diseases. Hepatobiliary Pancreat Dis Int 14(5):485–491.

Coombs J, van der List D, Wang GY, Chalupa LM (2006) Morphological properties of mouse retinal ganglion cells. Neuroscience 140:123–136.

Davies V, Votruba M (2006) Focus on molecules: the OPA1 protein. Exp Eye Res 83:1003–1004.

Davies VJ, Hollins AJ, Piechota MJ, Yip W, Davies JR, White KE, Nicols PP, Boulton ME, Votruba M (2007) Opa1 deficiency in a mouse model of autosomal dominant optic atrophy impairs mitochondrial morphology, optic nerve structure and visual function. Hum Mol Genet 16:1307–1318.

Delettre C, Lenaers G, Griffoin JM, Gigarel N, Lorenzo C, Belenguer P, Pelloquin L, Grosgeorge J, Turc-Carel C, Perret E, Astarie-Dequeker C, Lasquellec L, Arnaud B, Ducommun B, Kaplan J, Hamel CP (2000) Nuclear gene OPA1, encoding a mitochondrial dynamin-related protein, is mutated in dominant optic atrophy. Nat Genet 26:207–210.

Della Santina L, Inman DM, Lupien CB, Horner PJ, Wong RO (2013) Differential progression of structural and functional alterations in distinct retinal ganglion cell types in a mouse model of glaucoma. J Neurosci 33:17444–17457.

Di Prospero NA, Sumner CJ, Penzak SR, Ravina B, Fischbeck KH, Taylor JP (2007) Safety, tolerability, and pharmacokinetics of high-dose idebenone in patients with Friedreich ataxia. Arch Neurol 64:803–808.

Eiberg H, Kjer B, Kjer P, Rosenberg T (1994) Dominant optic atrophy (OPA1) mapped to chromosome 3q region. I. Linkage analysis. Hum Mol Genet 3:977–980.

El-Danaf RN, Huberman AD (2015) Characteristic patterns of dendritic remodeling in early-stage glaucoma: evidence from genetically identified retinal ganglion cell types. J Neurosci 35:2329–2343.

Elachouri G, Vidoni S, Zanna C, Pattyn A, Boukhaddaoui H, Gaget K, Yu-Wai-Man P, Gasparre G, Sarzi E, Delettre C, Olichon A, Loiseau D, Reynier P, Chinnery PF, Rotig A, Carelli V, Hamel CP, Rugolo M, Lenaers G (2011) OPA1 links human mitochondrial genome maintenance to mtDNA replication and distribution. Genome Res 21:12–20.

Erb M, Hoffmann-Enger B, Deppe H, Soeberdt M, Haefeli RH, Rummey C, Feurer A, Gueven N (2012) Features of idebenone and related short-chain quinones that rescue ATP levels under conditions of impaired mitochondrial complex I. PLoS ONE 7: e36153.

Esposti MD, Ngo A, Ghelli A, Benelli B, Carelli V, McLennan H, Linnane AW (1996) The interaction of Q analogs, particularly hydroxydecyl benzoquinone (idebenone), with the respiratory complexes of heart mitochondria. Arch Biochem Biophys 330:395–400.

Fiebiger SM, Bros H, Grobosch T, Janssen A, Chanvillard C, Paul F, Dorr J, Millward JM, Infante-Duarte C (2013) The antioxidant idebenone fails to prevent or attenuate chronic experimental

autoimmune encephalomyelitis in the mouse. J Neuroimmunol 262:66–71.
Formichi P, Radi E, Giorgi E, Gallus GN, Brunetti J, Battisti C, Rufa A, Dotti MT, Franceschini R, Bracci L, Federico A (2015) Analysis of opa1 isoforms expression and apoptosis regulation in autosomal dominant optic atrophy (ADOA) patients with mutations in the opa1 gene. J Neurol Sci 351:99–108.
Garcia-Segura LM, Perez-Marquez J (2014) A new mathematical function to evaluate neuronal morphology using the Sholl analysis. J Neurosci Methods 226:103–109.
Geifman N, Rubin E (2013) The mouse age phenome knowledgebase and disease-specific inter-species age mapping. PLoS ONE 8(12):e81114.
Giorgio V, Petronilli V, Ghelli A, Carelli V, Rugolo M, Lenaz G, Bernardi P (2012) The effects of idebenone on mitochondrial bioenergetics. Biochim Biophys Acta 1817:363–369.
Gkotsi D, Begum R, Salt T, Lascaratos G, Hogg C, Chau KY, Schapira AH, Jeffery G (2014) Recharging mitochondrial batteries in old eyes. Near infra-red increases ATP. Exp Eye Res 122:50–53.
Gueven N, Woolley K, Smith J (2015) Border between natural product and drug: comparison of the related benzoquinones idebenone and coenzyme Q10. Redox Biol 4:289–295.
Haefeli RH, Erb M, Gemperli AC, Robay D, Courdier Fruh I, Anklin C, Dallmann R, Gueven N (2011) NQO1-dependent redox cycling of idebenone: effects on cellular redox potential and energy levels. PLoS ONE 6:e17963.
Heitz FD, Erb M, Anklin C, Robay D, Pernet V, Gueven N (2012) Idebenone protects against retinal damage and loss of vision in a mouse model of Leber's hereditary optic neuropathy. PLoS ONE 7:e45182.
Hirai K, Hayako H, Kato K, Miyamoto M (1998) Idebenone protects hippocampal neurons against amyloid beta-peptide-induced neurotoxicity in rat primary cultures. Naunyn-Schmiedeberg's Arch Pharmacol 358:582–585.
Jaber S, Polster BM (2015) Idebenone and neuroprotection: antioxidant, pro-oxidant, or electron carrier? J Bioenerg Biomembr 47(1–2):111–118.
Jeon JH, Paik SS, Chun MH, Oh U, Kim IB (2013) Presynaptic localization and possible function of calcium-activated chloride channel anoctamin 1 in the mammalian retina. PLoS ONE 8:e67989.
King MS, Sharpley MS, Hirst J (2009) Reduction of hydrophilic ubiquinones by the flavin in mitochondrial NADH:ubiquinone oxidoreductase (Complex I) and production of reactive oxygen species. Biochemistry 48:2053–2062.
Klopstock T, Yu-Wai-Man P, Dimitriadis K, Rouleau J, Heck S, Bailie M, Atawan A, Chattopadhyay S, Schubert M, Garip A, Kernt M, Petraki D, Rummey C, Leinonen M, Metz G, Griffiths PG, Meier T, Chinnery PF (2011) A randomized placebo-controlled trial of idebenone in Leber's hereditary optic neuropathy. Brain 134:2677–2686.
Kutz K, Drewe J, Vankan P (2009) Pharmacokinetic properties and metabolism of idebenone. J Neurol 256(Suppl 1):31–35.
Lee SH, Park HJ, Chun HK, Cho SY, Cho SM, Lillehoj HS (2006) Dietary phytic acid lowers the blood glucose level in diabetic KK mice. Nutr Res 26:474–479.
Lenaers G, Hamel C, Delettre C, Amati-Bonneau P, Procaccio V, Bonneau D, Reynier P, Milea D (2012) Dominant optic atrophy. Orphanet J Rare Dis 7:46.
Lindsey JD, Duong-Polk KX, Hammond D, Chindasub P, Leung CK, Weinreb RN (2015a) Differential protection of injured retinal ganglion cell dendrites by brimonidine. Invest Ophthalmol Vis Sci 56:1789–1804.
Lindsey JD, Duong-Polk KX, Hammond D, Leung CK, Weinreb RN (2015b) Protection of injured retinal ganglion cell dendrites and unfolded protein response resolution after long-term dietary resveratrol. Neurobiol Aging 36:1969–1981.
Miyamoto M, Coyle JT (1990) Idebenone attenuates neuronal degeneration induced by intrastriatal injection of excitotoxins. Exp Neurol 108:38–45.
Newman NJ, Biousse V (2004) Hereditary optic neuropathies. Eye 18:1144–1160.
Olichon A, Landes T, Arnaune-Pelloquin L, Emorine LJ, Mils V, Guichet A, Delettre C, Hamel C, Amati-Bonneau P, Bonneau D, Reynier P, Lenaers G, Belenguer P (2007) Effects of OPA1 mutations on mitochondrial morphology and apoptosis: relevance to ADOA pathogenesis. J Cell Physiol 211:423–430.
Parkinson MH, Schulz JB, Giunti P (2013) Co-enzyme Q10 and idebenone use in Friedreich's ataxia. J Neurochem 126(Suppl 1):125–141.
Patten DA, Wong J, Khacho M, Soubannier V, Mailloux RJ, Pilon-Larose K, MacLaurin JG, Park DS, McBride HM, Trinkle-Mulcahy L, Harper ME, Germain M, Slack RS (2014) OPA1-dependent cristae modulation is essential for cellular adaptation to metabolic demand. EMBO J 33:2676–2691.
Piquereau J, Caffin F, Novotova M, Prola A, Garnier A, Mateo P, Fortin D, Huynh le H, Nicolas V, Alavi MV, Brenner C, Ventura-Clapier R, Veksler V, Joubert F (2012) Down-regulation of OPA1 alters mouse mitochondrial morphology, PTP function, and cardiac adaptation to pressure overload. Cardiovasc Res 94:408–417.
Porciatti V, Ventura LM (2012) Retinal ganglion cell functional plasticity and optic neuropathy: a comprehensive model. J Neuroophthalmol 32(4):354–358.
Quiros PM, Ramsay AJ, Sala D, Fernandez-Vizarra E, Rodriguez F, Peinado JR, Fernandez-Garcia MS, Vega JA, Enriquez JA, Zorzano A, Lopez-Otin C (2012) Loss of mitochondrial protease OMA1 alters processing of the GTPase OPA1 and causes obesity and defective thermogenesis in mice. EMBO J 31:2117–2133.
Sarzi E, Angebault C, Seveno M, Gueguen N, Chaix B, Bielicki G, Boddaert N, Mausset-Bonnefont AL, Cazevieille C, Rigau V, Renou JP, Wang J, Delettre C, Brabet P, Puel JL, Hamel CP, Reynier P, Lenaers G (2012) The human OPA1delTTAG mutation induces premature age-related systemic neurodegeneration in mouse. Brain 135:3599–3613.
Seo Y, Park J, Kim M, Lee HK, Kim JH, Jeong JH, Namkung W (2015) Inhibition of ANO1/TMEM16A chloride channel by idebenone and its cytotoxicity to cancer cell lines. PLoS ONE 10:e0133656.
Seznec H, Simon D, Monassier L, Criqui-Filipe P, Gansmuller A, Rustin P, Koenig M, Puccio H (2004) Idebenone delays the onset of cardiac functional alteration without correction of Fe-S enzymes deficit in a mouse model for Friedreich ataxia. Hum Mol Genet 13:1017–1024.
Sholl DA (1953) Dendritic organization in the neurons of the visual and motor cortices of the cat. J Anat 87:387–406.
Song Z, Chen H, Fiket M, Alexander C, Chan DC (2007) OPA1 processing controls mitochondrial fusion and is regulated by mRNA splicing, membrane potential, and Yme1L. J Cell Biol 178:749–755.
Suno M, Nagaoka A (1984) Inhibition of lipid peroxidation by a novel compound, idebenone (CV-2619). Jpn J Pharmacol 35:196–198.
Varanita T, Soriano ME, Romanello V, Zaglia T, Quintana-Cabrera R, Semenzato M, Menabo R, Costa V, Civiletto G, Pesce P, Viscomi C, Zeviani M, Di Lisa F, Mongillo M, Sandri M, Scorrano L (2015) The OPA1-dependent mitochondrial cristae remodeling pathway controls atrophic, apoptotic, and ischemic tissue damage. Cell Metab 21:834–844.
Votruba M, Fitzke FW, Holder GE, Carter A, Bhattacharya SS, Moore AT (1998a) Clinical features in affected individuals from 21 pedigrees with dominant optic atrophy. Arch Ophthalmol 116:351–358.
Votruba M, Moore AT, Bhattacharya SS (1998b) Clinical features, molecular genetics, and pathophysiology of dominant optic atrophy. J Med Genet 35:793–800.
Walter L, Nogueira V, Leverve X, Heitz MP, Bernardi P, Fontaine E (2000) Three classes of ubiquinone analogs regulate the mitochondrial permeability transition pore through a common site. J Biol Chem 275:29521–29527.

Williams PA, Morgan JE, Votruba M (2010) Opa1 deficiency in a mouse model of dominant optic atrophy leads to retinal ganglion cell dendropathy. Brain 133:2942–2951.

Williams PA, Piechota M, von Ruhland C, Taylor E, Morgan JE, Votruba M (2012) Opa1 is essential for retinal ganglion cell synaptic architecture and connectivity. Brain 135:493–505.

Wu C, Okar DA, Newgard CB, Lange AJ (2001) Overexpression of 6-phosphofructo-2-kinase/fructose-2, 6-bisphosphatase in mouse liver lowers blood glucose by suppressing hepatic glucose production. J Clin Investig 107:91–98.

Yu-Wai-Man P, Griffiths PG, Gorman GS, Lourenco CM, Wright AF, Auer-Grumbach M, Toscano A, Musumeci O, Valentino ML, Caporali L, Lamperti C, Tallaksen CM, Duffey P, Miller J, Whittaker RG, Baker MR, Jackson MJ, Clarke MP, Dhillon B, Czermin B, Stewart JD, Hudson G, Reynier P, Bonneau D, Marques Jr W, Lenaers G, McFarland R, Taylor RW, Turnbull DM, Votruba M, Zeviani M, Carelli V, Bindoff LA, Horvath R, Amati-Bonneau P, Chinnery PF (2010) Multi-system neurological disease is common in patients with OPA1 mutations. Brain 133:771–786.

Yu-Wai-Man P, Votruba M, Moore AT, Chinnery PF (2014) Treatment strategies for inherited optic neuropathies: past, present and future. Eye 28:521–537.

Zanna C, Ghelli A, Porcelli AM, Karbowski M, Youle RJ, Schimpf S, Wissinger B, Pinti M, Cossarizza A, Vidoni S, Valentino ML, Rugolo M, Carelli V (2008) OPA1 mutations associated with dominant optic atrophy impair oxidative phosphorylation and mitochondrial fusion. Brain 131:352–367.

Zhang Z, Wakabayashi N, Wakabayashi J, Tamura Y, Song WJ, Sereda S, Clerc P, Polster BM, Aja SM, Pletnikov MV, Kensler TW, Shirihai OS, Iijima M, Hussain MA, Sesaki H (2011) The dynamin-related GTPase Opa1 is required for glucose-stimulated ATP production in pancreatic beta cells. Mol Biol Cell 22:2235–2245.

(Accepted 19 January 2016)
(Available online 25 January 2016)